Organic & Biomolecular Chemistry

www.rsc.org/obc

Volume 10 | Number 29 | 7 August 2012 | Pages 5473–5660

ISSN 1477-0520

RSC Publishing

PAPER

Gevorg Sargsyan and Milan Balaz

Porphyrin–DNA conjugates: porphyrin induced adenine–guanine homoduplex stabilization and interduplex assemblies

Organic & Biomolecular Chemistry

Dynamic Article Links
View Online

Cite this: *Org. Biomol. Chem.*, 2012, **10**, 5533

www.rsc.org/obc

PAPER

Porphyrin–DNA conjugates: porphyrin induced adenine–guanine homoduplex stabilization and interduplex assemblies†

Gevorg Sargsyan and Milan Balaz*

Received 11th April 2012, Accepted 29th May 2012
DOI: 10.1039/c2ob25710f

DNA has found widespread uses as a nanosized scaffold for assembly of patterned multichomophoric nanostructures. Herein we report the synthesis, self-assembly, stability, and spectroscopic studies of short alternating non-self-complementary DNA sequences 5′-$(dGdA)_4$ and 5′-$(dAdG)_4$ with non-charged tetraarylporphyrins covalently linked to the 5′ position of deoxyadenosine or deoxyguanosine *via* a phosphate or amide linker. The linker, the metal in the porphyrin coordination center, and the neighboring nucleobase have very distinct effects on the duplex formation of porphyrin–deoxyguanosine–deoxyadenosine oligodeoxynucleotides. At ionic strength between 5 mM and 40 mM, free base trispyridylphenylporphyrin appended to the 5′ termini of 5′-$(dAdG)_4$ oligonucleotide *via* short non-polar amide linker served as a hydrophobic molecular cap inducing deoxyadenosine–deoxyguanosine antiparallel homoduplex. At ionic strength of ≥60 mM, the free base porphyrin functioned as a molecular 'glue' and induced the formation of porphyrin–DNA inter-homoduplex assemblies with characteristic tetrasignate CD Cotton effects in the porphyrin Soret band region. When the porphyrin cap was covalently attached to 5′ position of deoxyguanosine or deoxyadenosine *via* charged phosphate linker, no significant deoxyadenosine–deoxyguanosine hybridization was observed even at elevated ionic strengths.

Introduction

DNA is one of the most utilized templates in the search for new nanosized functional materials. Its broad uses result from well explored and predictable structural and self-assembly properties. The DNA molecular structure can be transformed into supramolecular multichromophoric helical ladders by means of non-covalent interactions.[1] Two complementary approaches with chromophores covalently incorporated into the DNA backbone or linked to DNA hydrogen bonding recognition units have been explored to assemble multichromophoric nanoarrays.[2–11] DNA nanomaterials can exhibit photophysical properties inaccessible from simple monomeric units providing proper arrangement of chromophores.[12] However, the possible applications of DNA in building new functional materials are limited by the chemical and physical characteristics of the natural DNA nucleosides. Most approaches rely on hydrogen bonding between adenine–thymine and guanine–cytosine base pairing along with stacking interactions between aromatic surfaces of nucleobases to assemble building blocks (*e.g.* chromophores, metals) into complex yet patterned nanostructures. The link between two nitrogenous bases of opposite complementarity represents not only the major strength but at the same time one of the bottlenecks in utilizing DNA as a supramolecular nanosized scaffold. Not surprisingly, the design and synthesis of new types of nucleobases (chemical analogues) with the ultimate goal of increasing the pool of base pairing combinations is a very active area of research.[13–20]

Small molecules can influence and alter DNA structure and stability. Four major DNA binding modes have been established: intercalation, minor groove binding, external stacking, and capping. Capping is characterized as a hydrophobic interaction of small aromatic molecules with the DNA terminus and is often promoted by covalently attaching the molecule to the proximity of the 5′ or 3′ DNA termini.[21,22] Although conventionally used to increase the base-paring fidelity of canonical hydrogen bonding in DNA and RNA recognition probes,[23] capping has a potential to be used in many other areas of DNA research. Berova and collaborators have reported that a non-charged tetraarylporphyrin cap covalently linked to the 5′ position of deoxyguanosine stabilized deoxyguanosine–deoxyadenosine (dG : dA) hydrogen bonding and a formation of a right-handed antiparallel homoduplex was confirmed by UV-vis absorption and circular dichroism spectroscopies.[24] Covalent modification of DNA terminus with aromatic molecules can represent a very attractive

Department of Chemistry, University of Wyoming, 1000 E. University ave., Laramie, WY 82071, USA. E-mail: mbalaz@uwyo.edu; Fax: +1 307 766-2807; Tel: +1 307 766-4330

† Electronic supplementary information (ESI) available: Circular dichroism, UV-vis absorption and emission spectra, MALDI-TOF spectra, and HPLC chromatograms for porphyrin–DNA conjugates. See DOI: 10.1039/c2ob25710f

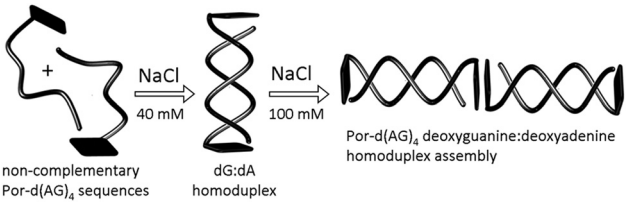

Fig. 1 Schematic representation of the formation of a porphyrin-capped adenine–guanine homoduplex (porphyrins are represented as black squares) in the presence of NaCl (40 mM) followed by a formation of supramolecular inter-duplex nanoassemblies upon further addition of NaCl (100 mM).

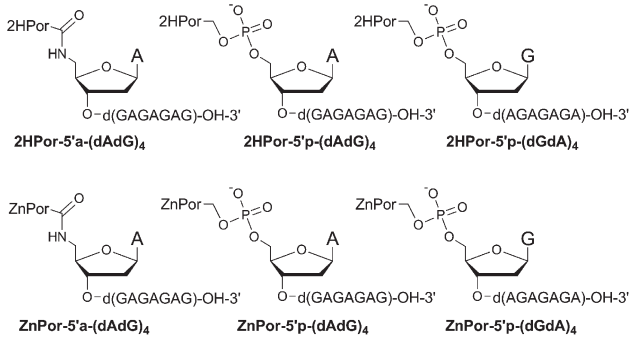

Chart 1 Structure of porphyrin–DNA 8-mer conjugates studied in this work.

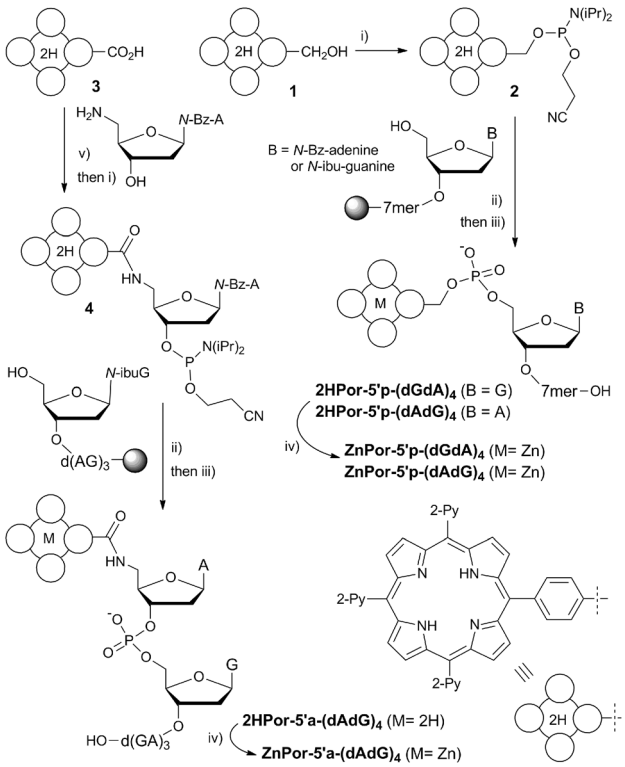

Scheme 1 Synthesis of free-base and zinc(II) DNA–porphyrin conjugates. Conditions: (i) 2-cyano-ethyl-*N*,*N*-diisopropylchloro-phosphoramidite, DIPEA, DCM; (ii) benzyl thiotetrazole in acetonitrile (activation reagent); (iii) iodine in pyridine–water–THF (oxidation reagent), then conc. NH_4OH (deprotection and cleavage); (iv) Zn $(OAc)_2{\cdot}2H_2O$; (v) DMAP, EDC, PyBOP, DCM.

method of increasing the pool of possible base pairing combinations without the necessity to design and synthesize new nucleobases. Additionally, caps can also serve as initiators that bring DNA duplexes together (DNA 'glue') in the form of supramolecular head-to-tail DNA oligomers.[25,26] One can envision capped non-self-complementary oligonucleotides that (a) self-assemble into homoduplexes with non-canonical base pairing as well as (b) form supramolecular inter-duplex assemblies all from building blocks that would not assemble without the proper cap.

In this article, we report the synthesis, self-assembly, and stability of short alternating non-self-complementary porphyrin–DNA conjugates of 5′-$(dGdA)_4$ and 5′-$(dAdG)_4$ explored by circular dichroism, UV-vis and fluorescence spectroscopies, and gel electrophoresis. The non-charged free-base- or zinc(II)-tetraarylporphyrins were covalently linked to the 5′ position of deoxyadenosine or deoxyguanosine *via* phosphate or amide linker. We evaluated the duplex formation with respect to the linker, metal in the porphyrin coordination center, the neighboring nucleobase, and the ionic strength. Only porphyrin appended to the 5′ termini of 5′-$(dAdG)_4$ oligonucleotide *via* short non-polar amide linker served as a molecular cap stabilizing adenine–guanine hydrogen bonding and inducing antiparallel deoxyadenosine–deoxyguanosine duplex at low ionic strengths (Fig. 1). Inter-duplex interactions induced by porphyrin stacking at higher ionic strength were also investigated.

Results and discussion

Synthesis of porphyrin–DNA conjugates

We have synthesized six porphyrin–DNA conjugates with the same number and type of nucleotides but varying in (1) nucleotide sequence, (2) linker between porphyrin and nucleotide, and (3) porphyrin metallation (Chart 1). Trispyridyl-monophenyl-porphyrin was covalently attached to the 5′ position of non-self-complementary guanine–adenine oligonucleotides using a phosphate linker (sequences 5′-$(dGdA)_4$ and 5′-$(dAdG)_4$) or an amide linker (sequence 5′-$(dAdG)_4$).[27] These linkers differ in length, flexibility, polarity, and their ability to induce metal coordination and hydrogen bonding, allowing us to elaborate on our previous results.[28,29]

For the phosphate linker, porphyrin benzyl alcohol **1** was first *O*-phosphitylated (Scheme 1).[30] Obtained phosphoramidite **2** was reacted with the 5′-hydroxy group of solid-supported 8-mers 5′-$(dGdA)_4$-ss or 5′-$(dAdG)_4$-ss under standard phosphoramidite conditions followed by oxidation, deprotection and cleavage from the resin to yield ***2HPor-5′p-(dGdA)$_4$*** and ***2HPor-5′p-(dAdG)$_4$***.[27,29] To attach the tetraarylporphyrin *via* amide linker, the porphyrin acid **3** was coupled to the 5′-amino *N*-benzoyl-deoxyadenosine.[31] The 3′-hydroxy group was then phosphitylated and reacted with the 5′-hydroxy of the solid supported 5′-dG$(dAdG)_3$-ss to give ***2HPor-5′a-(dAdG)$_4$*** (Scheme 1).

The zinc derivatives of porphyrin–DNA conjugates were prepared by metallation of the corresponding free-base precursors with $Zn(OAc)_2$. Crude porphyrin–ODNs were purified by a

Table 1 UV-vis absorption and emission properties of porphyrin–DNA conjugates

Conjugate	UV-vis absorption[a,b]	Emission[a,c]
2HPor-5′a-(dAdG)$_4$	255.4, 416.6 nm (5.41)	643.0, 705.0 nm
ZnPor-5′a-(dAdG)$_4$	256.2, 423.4 nm (5.60)	604.9, 654.0 nm
2HPor-5′p-(dAdG)$_4$	256.2, 416.7 nm (5.40)	645.9, 708.6 nm
ZnPor-5′p-(dAdG)$_4$	257.4, 423.4 nm (5.60)	607.4, 656.2 nm
2HPor-5′p-(dGdA)$_4$	256.8, 416.8 nm (5.45)	646.6, 709.3 nm
ZnPor-5′p-(dGdA)$_4$	257.3, 423.5 nm (5.50)	606.0, 655.7 nm

[a] Conditions: [Por–ODN] = 5.0 μM, Na-cacodylate buffer (1 mM, pH = 7.0). [b] DNA and Soret band absorption maxima (extinction coefficient, log ε). [c] Excited in the Soret band maximum.

reverse phase purification cartridge and their chemical identity and purity have been confirmed by MALDI-TOF mass spectrometry, HPLC, and UV-vis absorption and fluorescence spectroscopies. Analytical reverse phase HPLC showed the purity of all synthesized porphyrin–ODN conjugates to be >95% and did not show presence of side products or unreacted materials (ESI, Fig. S1–S16†). UV-vis absorption and emission characteristics of all six synthesized porphyrin–oligonucleotide conjugates are summarized in Table 1. Emission spectra were obtained by excitation in the Soret band, λ_{exc} = 417 nm for 2HPor–ODN derivatives and λ_{exc} = 425 nm for ZnPor–ODN conjugates (Fig. S6, S12, and S18†).

Circular dichroism, UV-vis and fluorescence spectroscopy

Alternating guanine–adenine DNA strands are known to form organized structures providing suitable conditions (low pH, high ionic strength, organic solvents) although their molecular structure is poorly characterized.[32–36] Circular dichroism is often employed to study the structural behavior of natural and synthetically modified oligonucleotides.[37–40] It has been shown that guanine–adenine self-organization gave rise to a positive Cotton effect in the CD spectrum at 265 nm.[24,33,41,42] The CD spectra of DNA–porphyrin conjugates ([Por–ODN] = 5.0 μM, DNA strand concentration) have been measured in Na-cacodylate buffer (1 mM, pH = 7.0) to explore their structural behavior and formation of helices. We have studied the effect of experimental conditions (temperature and ionic strength) as well as structural factors (linker, metallation of porphyrin, attached nucleoside) on the self-assembly of porphyrin-appended oligonucleotides and compared their behavior with natural porphyrin-free oligonucleotides under identical conditions. Analysis of CD spectra revealed that none of the six synthesized porphyrin–DNA conjugates showed guanine–adenine assembly in the absence of NaCl (low ionic strength conditions, I = 1 mM). Only very weak CD signals in the 220–300 nm region with no apparent 260 nm CD band have been observed (ESI, Fig. S87†). No significant induced CD signals have been observed in porphyrin Soret band absorption region (400–420 nm). Changing the temperature only caused small changes in the DNA or porphyrin spectral regions (Fig. S87†).

Porphyrin attached to deoxyadenosine *via* an amide linker

Free base porphyrin conjugate 2HPor-5′a-(dAdG)$_4$. CD spectra of **2HPor-5′a-(dAdG)$_4$** annealed at different ionic

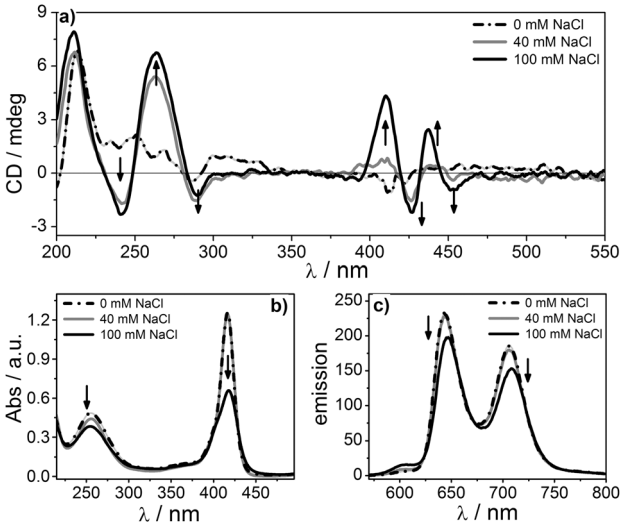

Fig. 2 Circular dichroism (a), UV-vis absorption (b), and emission (c) spectra of **2HPor-5′a-(dAdG)$_4$** at −2 °C annealed in the presence of 0 mM (black dash-dotted curve), 40 mM (grey solid curve), and 100 mM NaCl (black solid curve). Conditions: [Por–ODN] = 5.0 μM, Na-cacodylate buffer (1 mM, pH = 7.0). Annealing rate: from 60 °C to −2 °C at 0.5 °C min^{-1}.

strengths are shown in Fig. 2a. As can be seen, increasing the ionic strength from 1 mM to 40 mM NaCl had a dramatic effect on the CD spectrum of **2HPor-5′a-(dAdG)$_4$**. Strong positive CD Cotton effects at λ = 262 nm (+5.40 mdeg) and λ = 212 nm (+6.76 mdeg) and two weak negative CD bands at λ = 241.5 nm (−1.70 mdeg) and λ = 289 nm (−1.54 mdeg) were observed in the DNA absorption region of **2HPor-5′a-(dAdG)$_4$** upon slow annealing from 60 °C to −2 °C (Fig. 2a, grey solid curve). These A-DNA-like spectral features are similar to CD profile reported for the unmodified 5′-(dGdA)$_n$ sequences in the presence of ethanol or at low pH and have previously been reported for a different porphyrin–(dGdA)$_4$ conjugate.[24,33,41,42] Small bisignate CD signal with a negative CD Cotton effect at λ = 426 nm (−1.54 mdeg) and a positive Cotton effect at λ = 412 nm (+0.74 mdeg) was observed in the Soret region indicating a weak through-space exciton coupling between porphyrins oriented counterclockwise.

Increased ionic strength also influenced the UV-vis absorption and emission spectra of **2HPor-5′a-(dAdG)$_4$** (Fig. 2b and 2c). Upon annealing in the presence of 40 mM NaCl, the 256 nm absorbance band decreased from A = 0.484 to A = 0.440 (ΔH = −9%) while the Soret band absorption at 417 nm remained almost unchanged (ΔH < −1%; Fig. 2b, grey solid curve). The hypochromicity of the 260 nm band is associated with a single-to-double strand DNA transition. Fluorescence spectra of **2HPor-5′a-(dAdG)$_4$** are displayed in Fig. 2c. Excitation into the Soret band (λ_{exc} = 417 nm) in the absence of NaCl generated a fluorescence with maxima at 643 nm and 705 nm. Only minor changes in fluorescence intensities were observed upon the annealing of **2HPor-5′a-(dAdG)$_4$** with 40 mM NaCl (Fig. 2c, grey solid curve).

Our results suggested that at 40 mM NaCl, free-base porphyrin covalently attached to DNA served as a molecular cap and successfully promoted the formation of an ordered

antiparallel guanine–adenine duplex *via* stabilization of non-canonical dG : dA base pairing. To the contrary, uncapped 5′-$(dAdG)_4$ did not show self-association nor an increase of CD signal under identical conditions. Longer alternating dGdA sequences (*e.g.* 5′-$(dGdA)_{10}$) are known for their structural polymorphism and parallel and antiparallel duplexes, ordered single strands, triplexes, and hairpins have been reported in the presence of DMSO, ethanol, high salt, zinc(II), or low pH.[32–36] Since the formation and resulting CD signal of organized single strand and hairpin are concentration independent, we evaluated the effect of the concentration of **2HPor-5′a-$(dAdG)_4$** on the DNA CD signal (Fig. S88†). A decrease of the **2HPor-5′a-$(dAdG)_4$** concentration by half (from 5.0 μM to 2.5 μM) decreased the CD signals at 260 nm and 212 nm by 65% and 63% respectively, excluding the unimolecular assembly. Parallel duplex, triplex, and quadruplex of **2HPor-5′a-$(dAdG)_4$** would place two porphyrin units next to each other, causing a porphyrin stack. UV-vis and fluorescence spectra taken with 40 mM NaCl ruled out such an arrangement since only negligible absorption and emission changes have been detected in the Soret region (Fig. 2b,c). The antiparallel duplex is the most reasonable structure for **2HPor-5′a-$(dAdG)_4$** in the presence of 40 mM NaCl. Observed weak through-space exciton coupling between porphyrins provided additional evidence for the antiparallel duplex.

Annealing of **2HPor-5′a-$(dAdG)_4$** with 100 mM NaCl (instead of 40 mM NaCl) caused small changes in the DNA region of the CD spectrum and small increases (~20%) in intensity of Cotton effects at λ = 212, λ = 240 and λ = 262 nm were observed. CD signal in the Soret band region exhibited higher degree of complexity. A tetrasignate curve with two negative Cotton effects at λ = 452 nm (−0.92 mdeg) and λ = 427 nm (−2.20 mdeg) and two positive Cotton effects at λ = 437.5 nm (+2.45 mdeg) and λ = 410 nm (+4.34 mdeg) was detected (Fig. 2a, black solid curve). Multiple CD bands (*e.g.* trisignate and tetrasignate signals) in the Soret band region have been observed when two and more porphyrins were held tightly together in a helical assembly mediated by π–π stacking.[43–47] It has previously been shown that multisignate CD signals in the porphyrin region originated from strong electronic interaction between helically stacked porphyrins of at least two porphyrin–DNA conjugates.[28] Conversely, the CD of the porphyrin-free 5′-$(dAdG)_4$ annealed with 100 mM NaCl showed the expected weak CD spectrum with negative bands at 285 nm and 261 nm and a positive band at 246 nm confirming the absence of guanine–adenine hybridization (Fig. S79†). In the UV-vis absorption spectrum, increase of ionic strength to 100 mM NaCl caused a drop of 260 nm band to A = 0.382 (ΔH = −21%; Fig. 2b, black solid curve). Soret band experienced significant hypochromicity upon annealing the **2HPor-5′a-$(dAdG)_4$** with 100 mM NaCl and the absorption decreased to A = 0.656 (ΔH = −47%, Fig. 2a, black solid curve). The fluorescence intensity decreased by ~15% (Fig. S28†) at 100 mM NaCl. We have recently reported similar absorption and emission behavior for the salt-induced intermolecular porphyrin–porphyrin interactions of an oligoadenine conjugate **2HPor-5′a-$(dA)_8$**.[30] Absorption and emission data confirmed the porphyrin-mediated inter duplex interactions of **2HPor-5′a-$(dAdG)_4$**.

Annealing UV-vis experiments (from +60 °C to −2 °C, cooling rate 1 °C min^{-1}) of **2HPor-5′a-$(dAdG)_4$** in the presence of 100 mM NaCl yielded low-cooperative melting curves with the melting temperature T_m of +15.8 °C (260 nm). Variable temperature CD experiments of **2HPor-5′a-$(dAdG)_4$** (from +60 °C to −2 °C, cooling rate 0.5 °C min^{-1}) in the presence of 100 mM NaCl demonstrated that the DNA CD signal (260 nm CD band) started to appear at 38 °C whereas a temperature below 25 °C was needed for the CD signal in Soret region (260 nm CD band) to appear (Fig. 3). The CD results suggested that dG : dA duplex is formed first followed by formation of supramolecular inter-duplex porphyrin–DNA oligomers. Porphyrins appended at oligonucleotide terminus thus served as guanine–adenine molecular cap and as DNA 'glue' between two guanine–adenine duplexes. NaCl titration experiments of **2HPor-5′a-$(dAdG)_4$** revealed a transition of random coiled single strand (0 mM NaCl) to organized duplex (from 5 mM to 40 mM) to inter-duplex assemblies (≥60 mM) (Fig. S89†). The presence of one isosbestic point in the DNA region of the CD spectrum (252 nm) confirmed the equilibrium between two DNA forms, single-stranded and double-stranded. The three-step transition was observed in the Soret region where a negative exciton coupled CD signal that appeared at 5 mM NaCl (single to double strand transition) transformed into the tetrasignate CD signal above 40 mM NaCl (porphyrin promoted duplex association). Addition of equimolar amount of a complementary DNA sequence, 5′-$(dCdT)_4$ to **2HPor-5′a-$(dAdG)_4$** in the presence of 100 mM NaCl at −2 °C caused fast disappearance of the 410 nm CD band as can be seen in the Fig. S90.† The resulting CD spectrum showed similar features as the spectrum obtained by mixing equimolar amounts of **2HPor-5′a-$(dAdG)_4$** and 5′-$(dCdT)_4$ at 60 °C followed by slow annealing to −2 °C (cooling rate 0.5 °C min^{-1}).

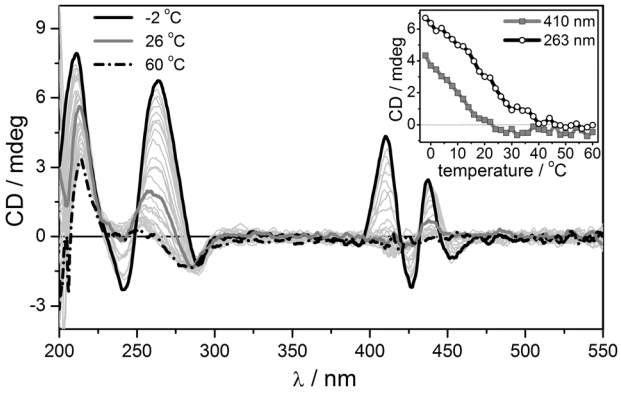

Fig. 3 Variable temperature CD spectra of **2HPor-5′a-$(dAdG)_4$** in the presence of 100 mM NaCl. The sample was cooled from 60 °C to −2 °C at 1 °C min^{-1} and CD spectrum was recorded every 2 °C. Inset: CD signal at 410 nm and 263 nm as a function of temperature. Conditions: [Por–ODN] = 5.0 μM, Na-cacodylate buffer (1 mM, pH = 7.0). Annealing rate: from 60 °C to −2 °C at 0.5 °C min^{-1}.

Zinc(II) porphyrin conjugate ZnPor-5′a-$(dAdG)_4$. Fig. 4a shows CD spectra of **ZnPor-5′a-$(dAdG)_4$** annealed from 60 °C to −2 °C in the absence of NaCl (black dash-dotted curve) and in the presence of 40 mM (grey solid curve) and 100 mM NaCl (black solid curve). Annealing in the presence of 40 mM NaCl gave rise to two negative CD bands at λ = 289 nm (−0.92 mdeg)

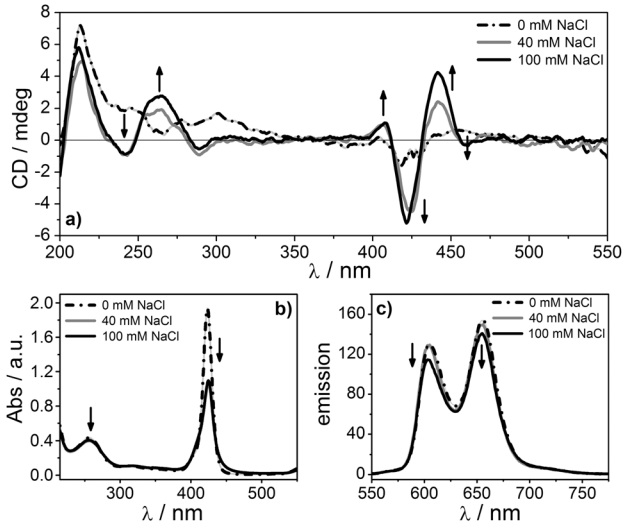

Fig. 4 Circular dichroism (a), UV-vis absorption (b), and emission (c) spectra of **ZnPor-5′a-(dAdG)$_4$** in the presence of 0 mM (black dash-dotted curve), 40 mM (grey solid curve), and 100 mM (black solid curve) NaCl. Conditions: [Por–ODN] = 5.0 μM, Na-cacodylate buffer (1 mM, pH = 7.0). Cooling rate: 0.5 °C min^{-1} from 60 °C to −2 °C.

and λ = 243 nm (−0.96 mdeg) and a positive CD band at λ = 265 nm (1.92 mdeg; Fig. 4a, grey solid curve). Unlike **2HPor-5′-a-(dAdG)$_4$**, **ZnPor-5′a-(dAdG)$_4$** gave rise to the tetrasignate CD profile in the Soret region already at 40 mM NaCl with two negative Cotton effects (−0.24 mdeg at λ = 459 nm and −4.49 mdeg at λ = 425 nm) and two positive Cotton effects (2.41 mdeg at λ = 442 nm and 0.96 mdeg at λ = 405.5 nm). Annealing of **ZnPor-5′a-(dAdG)$_4$** in the presence of 100 mM NaCl generated a more pronounced CD spectrum with similar profile as the **2HPor-5′a-(dAdG)$_4$** (Fig. 4a, black solid curve).

Fig. 4b and 4c show the effect of ionic strength on UV-vis absorption and emission spectra of the **ZnPor-5′a-(dAdG)$_4$**. The increase of ionic strength from 1 mM to 40 mM and then to 100 mM caused a decrease of 256 nm absorbance band from A = 0.432 to A = 0.398 and then to 0.406, respectively. The Soret band dropped from A = 1.923 to A = 1.055 and A = 1.095 ($\Delta H \sim -20\%$; Fig. 4b). Excitation into the Soret band in the absence of NaCl (λ_{exc} = 425 nm) generated an emission spectrum with maxima at 605 nm and 655 nm (Fig. 4c, black dash-dotted curve). Annealing with 40 mM NaCl caused only minor changes in the emission spectrum (Fig. 4c, grey solid curve) whereas in the presence of 100 mM the intensity of emission spectrum decreased by ∼9% (black solid curve). Variable temperature UV-vis spectra of **ZnPor-5′a-(dAdG)$_4$** showed strong hypochromicity of the Soret band. In the absence of NaCl, the Soret band signal at 424.6 nm dropped from A = 1.89 to A = 1.46 (22% hypochromicity) by decreasing the temperature from 60 °C to −2 °C at 0.5 °C min^{-1}. In the presence of 40 mM NaCl, the Soret band absorption decreased from A = 1.65 to A = 1.06 (35% hypochromicity) whereas in the presence of 100 mM NaCl the absorption changed from A = 1.51 to A = 1.09 (28% hypochromicity).

ZnPor-5′a-(dAdG)$_4$ exhibited a smaller degree of adenine–guanine dimerization and produced a smaller increase of the positive CD band at 263 nm than its free-base counterpart

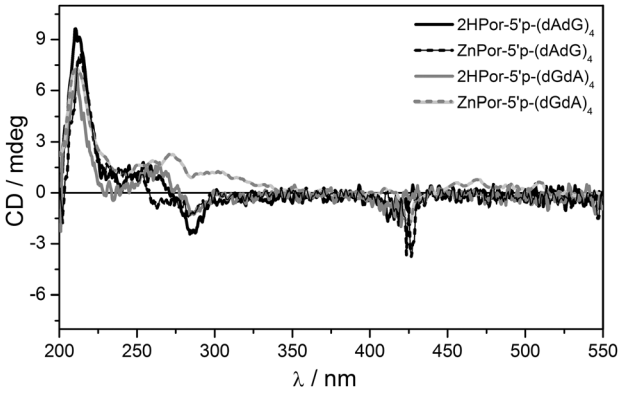

Fig. 5 Circular dichroism spectra of **2HPor-5′p-(dAdG)$_4$** (black solid curve), **ZnPor-5′p-(dAdG)$_4$** (black dashed curve), **2HPor-5′p-(dGdA)$_4$** (grey solid curve), **ZnPor-5′p-(dGdA)$_4$** (grey dashed curve) in the presence of 40 mM NaCl. Conditions: [Por–ODN] = 5.0 μM, Na-cacodylate buffer (1 mM, pH = 7.0), annealing rate 0.5 °C min^{-1} from 60 °C to −2 °C.

2HPor-5′a-(dAdG)$_4$. Zinc porphyrins have been shown to have one axial water molecule coordinated to the zinc atom in aqueous solutions. The axial ligand together with increased hydrophilicity and nonplanarity of zinc(II)porphyrin (zinc atom is ∼0.2 Å above the N4 plane) most likely hindered effective π–π interactions between zinc porphyrin and the adjacent adenine–guanine base pair.[48] Annealing CD experiments (cooling rate 0.5 °C min^{-1}) in the presence of 100 mM NaCl revealed that the DNA (260 nm) and Soret band (441 nm) CD signals started to appear when the temperature decreased below 30 °C (Fig. S35†). The spectroscopic data suggested that in comparison to the metal free **2HPor-5′a-(dAdG)$_4$**, the **ZnPor-5′a-(dAdG)$_4$** has higher tendency towards intermolecular porphyrin–porphyrin interactions (*i.e.* yielding Soret band CD signal at lower ionic strength) than towards the intramolecular capping.

Porphyrin attached to DNA *via* a phosphate linker

CD spectra of porphyrin–DNA conjugates with porphyrin attached to the 5′ position of deoxyadenosine (**2HPor-5′p-(dAdG)$_4$** and **ZnPor-5′p-(dAdG)$_4$**) showed little changes in the DNA region upon annealing in the presence of 40 mM NaCl whereas negative CD bands have been observed in the Soret region (Fig. 5 and S51†).

Upon increasing the ionic strength to 100 mM NaCl, a small positive Cotton effect at 262 nm was observed for **2HPor-5′p-(dAdG)$_4$** whereas **ZnPor-5′p-(dAdG)$_4$** did not yield any increase of the DNA CD signal. Conversely, UV-vis absorption spectra displayed similar behavior as porphyrin–DNA conjugates with the amide linker. In the case of **2HPor-5′p-(dAdG)$_4$** (Fig. S40†), the Soret band intensity at −2 °C dropped from A = 1.27 (sample annealed in the absence of NaCl) to A = 1.15 (annealed with 40 mM) and then further to A = 0.93 (annealed with 100 mM). Similarly, the Soret band absorption of **ZnPor-5′-p-(dAdG)$_4$** decreased from A = 2.02 (no NaCl) to A = 1.64 (100 mM NaCl, Fig. S49†). Non-denaturing polyacrylamide gel electrophoresis (PAGE) confirmed different self-assembly

behavior of the amide-linked **2HPor-5′a-(dAdG)$_4$** and phosphate-linked **2HPor-5′p-(dAdG)$_4$** (Fig. S91†). The migration of the **2HPor-5′a-(dAdG)$_4$** was slower than the migration of the **2HPor-5′p-(dAdG)$_4$** in 1 mM Na-cacodylate buffer with 40 mM NaCl indicating the assembly formation of the former.

The effects of ionic strength on CD spectra of porphyrin–DNA conjugates **2HPor-5′p-(dGdA)$_4$** and **ZnPor-5′p-(dGdA)$_4$** with porphyrin covalently attached to the 5′ position of deoxyguanosine are displayed in Fig. 5 and Fig. S57–S72.† Small positive CD bands were observed at 263 nm upon annealing the **2HPor-5′p-(dGdA)$_4$** with 40 mM and 100 mM NaCl. Higher ionic strength (100 mM NaCl) was necessary to induce an increase of the 263 nm CD band with **ZnPor-5′p-(dGdA)$_4$**. CD spectra of **2HPor-5′p-(dGdA)$_4$** did not exhibit induced signal in the Soret region at any ionic strength (Fig. S63†). On the other hand, small negative Cotton effects were observed in the Soret region (425 nm) of **ZnPor-5′p-(dGdA)$_4$** CD spectra under all tested ionic strengths (Fig. S69, S72†).

The data indicated that phosphate appended 2H-porphyrin and zinc(II)porphyrin did not provide efficient capping and stabilization of adenine–guanine base pairs. Only a small increase of 263 nm CD band was observed for **2HPor-5′p-(dAdG)$_4$** and **2HPor-5′p-(dGdA)$_4$** at 40 mM and 100 mM NaCl (Fig. 5 and ESI†). Zinc(II)derivatives **ZnPor-5′p-(dAdG)$_4$** and **ZnPor-5′p-(dGdA)$_4$** did not show any degree of adenine–guanine duplex stabilization. No inter-duplex interactions were detected for any of the phosphate appended porphyrin–DNA conjugates as judged by lack of tetrasignate CD Cotton effects in the Soret band region. Studies are ongoing to explain why the charged and more flexible phosphate linker does not allow for efficient capping of guanine–adenine homoduplex. Fig. 6 summarizes the adenine–guanine duplex formation as recorded by the increase of the CD band at 263 nm. Free base-porphyrin–DNA conjugate **2HPor-5′a-(dAdG)$_4$** with porphyrin appended to adenine *via* amide linker exhibited the largest chirality augmentation. The CD signal of **2HPor-5′a-(dAdG)$_4$** was 2–5 times stronger than CD signal of other porphyrin conjugates under identical experimental conditions.

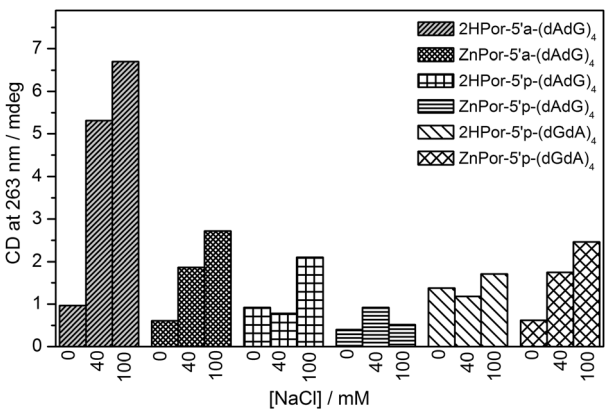

Fig. 6 The intensity of the 263 nm CD band of porphyrin–DNA conjugates in the presence of 0 mM, 40 mM, and 100 mM of NaCl. Conditions: [Por–ODN] = 5.0 μM, Na-cacodylate buffer (1 mM, pH = 7.0).

Conclusions

Our results illustrated the power of porphyrins to induce the formation of DNA nanoassemblies. Covalently attached porphyrin was successfully used as a DNA molecular cap to assemble non-self-complementary adenine–guanine DNA strands into antiparallel homoduplexes and at the same time served as the DNA 'glue' to form interduplex nanostructures.[25] Linker and molecular cap together with environmental conditions played a vital role in successful adenine–guanine hybridization. At ionic strengths of 5 mM to 40 mM and at temperatures below 40 °C, free base trispyridylphenylporphyrin appended to the 5′-DNA terminus of 5′-(dAdG)$_4$ *via* short non-polar amide linker served as a hydrophobic molecular cap inducing deoxyadenosine–deoxyguanine antiparallel duplex. At ionic strength of 100 mM, the free base porphyrin functioned as molecular 'glue' and promoted the formation of porphyrin–DNA interduplex assemblies with very characteristic tetrasignate CD Cotton effects in the Soret band region. Zinc porphyrin generated a smaller degree of capping because of the axial water ligand. When the porphyrin was covalently attached to 5′ position of deoxyguanosine or deoxyadenosine *via* charged, more flexible phosphate linker no significant deoxyadenosine–deoxyguanine hybridization was observed even at 100 mM NaCl. Capping could potentially lead to preparation of functional supramolecular inter-DNA polymers formed by self-assembly of non-complementary oligonucleotides with proper terminus capping.

Experimental

All commercially available reagents were used as received without purification unless otherwise stated. Dichloromethane (DCM) and tetrahydrofuran (THF) were dried by distillation from calcium hydride and lithium aluminum hydride, respectively. 2-Cyanoethyl *N*,*N*-diisopropylchloro-phosphoramidite was purchased from Sigma-Aldrich. Oligonucleotides attached to 1000 Å controlled pore glass (CPG) solid-support cartridges were purchased from Alpha DNA. DNA purification cartridges (Puri-Pak 0.2 μM), activation reagent (benzyl thiotetrazole in acetonitrile) and oxidation solution (0.02 M iodine in pyridine–water–tetrahydrofuran) were purchased from ChemGenes Corporation. MALDI-TOF MS spectra measurements were performed on a Applied Biosystems Voyager DE STR spectrometer using the 3-hydroxypicolinic acid (3-HPA) with ammonium dibasic citrate as the matrix using external standards.

Porphyrin and porphyrin–oligonucleotides synthesis

Porphyrin alcohol **1**, porphyrin phosphoramidites **2** and **4**, and 5′-aminodeoxyadenosine were synthesized according to previously reported procedures.[27,29,49] Porphyrin–phosphoramidite **2** was prepared from a porphyrin alcohol **1** (8.0 mg, 0.012 mmol) using previously reported procedure[30] and immediately mixed with solid-supported sequences 5′-OH-(dGdA)$_4$-ss or 5′-OH-(dAdG)$_4$-ss in dry DCM (0.5 ml) and activation reagent (0.5 ml, 0.45 M tetrazole in acetonitrile). The suspension was stirred for 1 h at room temperature in the dark. The 3′-phosphitylated porphyrin-deoxyadenosine **4** was reacted with

7-mer 5′-dG-$(dAdG)_3$-ss under identical conditions. The red-colored resin was then washed with DCM (6 ml), acetonitrile (6 ml), and THF (6 ml), then treated with the oxidation solution for 20 min. The solution was filtered off and the resin washed exhaustively. The deprotection and cleavage of DNA–porphyrin conjugate from the resin was achieved by concentrated ammonia at room temperature in the dark for 24 h. The red supernatant containing cleaved oligonucleotides was carefully removed and purified by oligonucleotide purification cartridge. The cartridge was pre-equilibrated with acetonitrile (4 ml) and TEAA (1 M, 6 ml). A 1 : 1 aqueous ammonia solution of porphyrin–DNA conjugate was loaded onto the cartridge, washed with ammonia (3%, 6 ml) and deionized water (6 ml). The porphyrin–DNA conjugates were eluted with a 50% aqueous acetonitrile. Zinc conjugates were prepared from the corresponding free base precursors. $Zn(OAc)_2$ (100 mM, 0.5 ml) was added to a free base porphyrin–DNA conjugate dissolved in water and the resulting solution was stirred at 50 °C for 30 min. Zn-porphyrin–DNA conjugates were purified by reverse phase purification cartridge as described for their free-base counterparts. The chemical identity and purity of porphyrin–DNA conjugates have been confirmed by MALDI-TOF mass spectrometry, reverse phase HPLC, and UV-vis absorption and fluorescence spectroscopies. Analytical reverse phase HPLC showed the purity of all synthesized porphyrin–DNA conjugates to be >95% (ESI, Fig. S1–S16†). MALDI-TOF mass spectrometry corroborated the purity and did not show presence of side products. **2HPor-5′p-$(dAdG)_4$**, $[M - H]^+$ requires 3216.692, found 3216.692; **ZnPor-5′p-$(dAdG)_4$**, $[M - H]^+$ requires 3278.605, found 3279.031; **2HPor-5′p-$(dGdA)_4$**, $[M - H]^+$ requires 3216.692, found 3217.431; **ZnPor-5′p-$(dGdA)_4$**, $[M - H]^+$ requires 3278.605, found 3280.707; **2HPor-5′a-$(dAdG)_4$**, $[M - H]^+$ requires 3149.721, found 3149.024; **ZnPor-5′a-$(dAdG)_4$**, $[M - H]^+$ requires 3211.634, found 3211.046 (ESI, Fig. S1–S16†).

Spectroscopy

Water was obtained from Milli-Q system with a resistivity of 18.2 MΩ cm. Porphyrin substituted oligonucleotides were dissolved in sodium cacodylate buffer (1 mM, pH 7.0). Concentrations were quantified at 20 °C by a Jasco V-650 UV-vis absorption spectrometer and are reported as DNA strand concentrations. Sodium chloride concentrations were increased by adding NaCl directly to the cell. Circular dichroism spectra were recorded on a Jasco J-815 spectropolarimeter equipped with a single cell Peltier temperature control system. Conditions were as follows: scanning speed 100 nm min^{-1}, data pitch 0.5 nm, DIT 2 s, and bandwidth 1 nm. Each CD spectrum was an average of at least two scans. UV-vis absorption spectra were collected at 20 °C using a Jasco V-650 UV-vis double beam spectrophotometer equipped with a single position Peltier temperature control system. Emission spectra were recorded on a Varian Cary Eclipse fluorescence spectrophotometer equipped with a Peltier temperature control system. Conditions were as follows: excitation slit 5 nm, emission slit 5 nm, scan rate 600 nm min^{-1}. A quartz cuvette with a 1 cm path length was used for all spectroscopic experiments. In a typical experiment, 33 μL of porphyrin–DNA conjugate stock solution (240 μM, Na-cacodylate buffer) was added to the cuvette containing 1567 μL of Na-cacodylate buffer with or without NaCl. The solution was heated and kept at 60 °C for 20 min and cooled to −2 °C at 0.5 °C min^{-1}.

Gel electrophoresis

Non-denaturing polyacrylamide gel electrophoresis was performed in a Bio-Rad mini-PROTEAN Tetra system. Gels (20%, 29 : 1 monomer : bis ratio) were prepared by mixing 40% acrylamide : bis (29 : 1, 5 ml), deionized water (2.9 ml), 50 mM Na-cacodylate buffer with 200 mM NaCl (2 ml), 10% w/v ammonium persulfate (100 μl), and TMEDA (8 μL). Gels were run in Na-cacodylate buffer (1 mM, pH = 7.0) with 40 mM NaCl for 8 h at 30 mA at 0 °C. Ultraviolet lamp (λ = 365 nm) was used to visualize porphyrin–DNA conjugates.

Acknowledgements

We thank University of Wyoming Start-up funds and the School of Energy Resources (Graduate Assistantship for GS).

Notes and references

1 R. Varghese and H. A. Wagenknecht, *Chem. Commun.*, 2009, 2615.
2 E. Mayer-Enthart and H. A. Wagenknecht, *Angew. Chem., Int. Ed.*, 2006, **45**, 3372.
3 L. A. Fendt, I. Bouamaied, S. Thoni, N. Amiot and E. Stulz, *J. Am. Chem. Soc.*, 2007, **129**, 15319.
4 T. Nguyen, A. Brewer and E. Stulz, *Angew. Chem., Int. Ed.*, 2009, **48**, 1974.
5 V. L. Malinovskii, F. Samain and R. Haner, *Angew. Chem., Int. Ed.*, 2007, **46**, 4464.
6 R. Haner, F. Samain and V. L. Malinovskii, *Chem.–Eur. J.*, 2009, **15**, 5701.
7 A. W. I. Stephenson, N. Bomholt, A. C. Partridge and V. V. Filichev, *ChemBioChem*, 2010, **11**, 1833.
8 M. Balaz, A. E. Holmes, M. Benedetti, P. C. Rodriguez, N. Berova, K. Nakanishi and G. Proni, *J. Am. Chem. Soc.*, 2005, **127**, 4172.
9 C. Brotschi, G. Mathis and C. J. Leumann, *Chem.–Eur. J.*, 2005, **11**, 1911.
10 P. G. A. Janssen, J. Vandenbergh, J. L. J. van Dongen, E. W. Meijer and A. Schenning, *J. Am. Chem. Soc.*, 2007, **129**, 6078.
11 R. Iwaura, F. J. M. Hoeben, M. Masuda, A. Schenning, E. W. Meijer and T. Shimizu, *J. Am. Chem. Soc.*, 2006, **128**, 13298.
12 H. Kashida, K. Sekiguchi, X. Liang and H. Asanuma, *J. Am. Chem. Soc.*, 2010, **132**, 6223.
13 D. W. Jiang and F. Seela, *J. Am. Chem. Soc.*, 2010, **132**, 4016.
14 F. Wojciechowski and C. J. Leumann, *Chem. Soc. Rev.*, 2011, **40**, 5669.
15 M. Berger, S. D. Luzzi, A. A. Henry and F. E. Romesberg, *J. Am. Chem. Soc.*, 2002, **124**, 1222.
16 J. C. Delaney, J. Gao, H. Liu, N. Shrivastav, J. M. Essigmann and E. T. Kool, *Angew. Chem., Int. Ed.*, 2009, **48**, 4524.
17 A. A. Henry, C. Yu and F. E. Romesberg, *J. Am. Chem. Soc.*, 2003, **125**, 9638.
18 A. M. Leconte, G. T. Hwang, S. Matsuda, P. Capek, Y. Hari and F. E. Romesberg, *J. Am. Chem. Soc.*, 2008, **130**, 2336.
19 J. Stambasky, M. Hocek and P. Kocovsky, *Chem. Rev.*, 2009, **109**, 6729.
20 F. Seela and H. Debelak, *Nucleic Acids Res.*, 2000, **28**, 3224.
21 J. Tuma, R. Paulini, J. A. Rojas Stutz and C. Richert, *Biochemistry*, 2004, **43**, 15680.
22 S. Narayanan, J. Gall and C. Richert, *Nucleic Acids Res.*, 2004, **32**, 2901.
23 S. Egetenmeyer and C. Richert, *Chem.–Eur. J.*, 2011, **17**, 11813.
24 M. Balaz, B. C. Li, G. A. Ellestad and N. Berova, *Angew. Chem., Int. Ed.*, 2006, **45**, 3530.
25 D. Baumstark and H. A. Wagenknecht, *Angew. Chem., Int. Ed.*, 2008, **47**, 2612.
26 F. Menacher, V. Stepanenko, F. Würthner and H.-A. Wagenknecht, *Chem.–Eur. J.*, 2011, **17**, 6683.

27 M. Balaz, A. E. Holmes, M. Benedetti, G. Proni and N. Berova, *Bioorg. Med. Chem.*, 2005, **13**, 2413.
28 A. Mammmana, G. Pescitelli, T. Asakawa, S. Jockusch, A. G. Petrovic, R. R. Monaco, R. Purrello, N. J. Turro, K. Nakanishi, G. A. Ellestad, M. Balaz and N. Berova, *Chem.–Eur. J.*, 2009, **15**, 11853.
29 A. Mammana, T. Asakawa, K. Bitsch-Jensen, A. Wolfe, S. Chaturantabut, Y. Otani, X. X. Li, Z. M. Li, K. Nakanishi, M. Balaz, G. A. Ellestad and N. Berova, *Bioorg. Med. Chem.*, 2008, **16**, 6544.
30 G. Sargsyan, B. L. MacLeod, U. Tohgha and M. Balaz, *Tetrahedron*, 2012, **68**, 2093–2099.
31 X. Hu, M. T. Tierney and M. W. Grinstaff, *Bioconjugate Chem.*, 2001, **13**, 83.
32 J. Kypr and M. Vorlickova, *Biopolymers*, 2001, **62**, 81.
33 M. Vorlickova, I. Kejnovska, J. Kovanda and J. Kypr, *Nucleic Acids Res.*, 1999, **27**, 581.
34 M. Ortizlombardia, R. Eritja, F. Azorin, J. Kypr, I. Tejralova and M. Vorlickova, *Biochemistry*, 1995, **34**, 14408.
35 N. G. Dolinnaya and J. R. Fresco, *Proc. Natl. Acad. Sci. U. S. A.*, 1992, **89**, 9242.
36 I. Kejnovska, J. Kypr, J. Vondruskova and M. Vorlickova, *Biopolymers*, 2007, **85**, 19.
37 J. Kypr, I. Kejnovska, D. Renciuk and M. Vorlickova, *Nucleic Acids Res.*, 2009, **37**, 1713.
38 C. Johnson, CD of Nucleic Acids, in *Circular Dichroism, Principles and Applications*, ed. N. Berova, K. Nakanishi and R. W. Woody, New York, 2000, p. 703.
39 M. Balaz, K. Bitsch-Jensen, A. Mammana, G. A. Ellestad, K. Nakanishi and N. Berova, *Pure Appl. Chem.*, 2007, **79**, 801.
40 M. Balaz, B. C. Li, J. D. Steinkguger, G. A. Ellestad, K. Nakanishi and N. Berova, *Org. Biomol. Chem.*, 2006, **4**, 1865.
41 I. Kejnovska, J. Kypr and M. Vorlickova, *Chirality*, 2003, **15**, 584.
42 M. Vorlickova, I. Kejnovska, J. Kovanda and J. Kypr, *Nucleic Acids Res.*, 1998, **26**, 1509.
43 G. Pescitelli, S. Gabriel, Y. K. Wang, J. Fleischhauer, R. W. Woody and N. Berova, *J. Am. Chem. Soc.*, 2003, **125**, 7613.
44 G. Bringmann, D. C. G. Gotz, T. A. Gulder, T. H. Gehrke, T. Bruhn, T. Kupfer, K. Radacki, H. Braunschweig, A. Heckmann and C. Lambertt, *J. Am. Chem. Soc.*, 2008, **130**, 17812.
45 M. Ikeda, S. Shinkai and A. Osuka, *Chem. Commun.*, 2000, 1047.
46 M. Takeuchi, T. Imada and S. Shinkai, *Bull. Chem. Soc. Jpn.*, 1998, **71**, 1117.
47 L. Palivec, M. Urbanova and K. Volka, *J. Pept. Sci.*, 2005, **11**, 536.
48 A. H. Shelton, A. Rodger and D. R. McMillin, *Biochemistry*, 2007, **46**, 9143.
49 X. Hu, M. T. Tierney and M. W. Grinstaff, *Bioconjugate Chem.*, 2002, **13**, 83.

